Available online at www.sciencedirect.com

SCIENCE DIRECT®

Journal of Petroleum Science and Engineering 46 (2005) 283–297

JOURNAL OF PETROLEUM SCIENCE & ENGINEERING

www.elsevier.com/locate/petrol

Depletion oil recovery for systems with widely varying initial composition☆

Kameshwar Singh[a,*], Øivind Fevang[a], Curtis H. Whitson[b]

[a]*PERA, Norway*
[b]*NTNU/PERA, Norway*

Received 25 February 2004; accepted 27 January 2005

Abstract

The principal depletion drive mechanism is the expansion of oil and gas initially in the reservoir—neglecting water influx. The main factors in depletion drive reservoir performance are total cumulative compressibility, determined mostly by initial composition (gas–oil ratio), saturation pressure, PVT properties, and relative permeability. In this paper, we systematically study the effect of initial composition on oil recovery, all other parameters held constant. We also evaluate other aspects of reservoir performance, but the main emphasis is surface oil recovery including condensate.

To analyze the effect of initial composition, a series of fluid systems was selected by a recombination of separator samples at varying gas–oil ratios. The systems ranged from low-GOR oils to high-GOR gas condensates, with a continuous transition from gas to oil through a critical mixture.

Black oil and compositional material balance calculations, 2D fine-grid, and 3D coarse-grid models have been used to investigate the effect of initial fluid composition on reservoir depletion performance. Systematic variation of relative permeabilities was also used to map the range of fluid systems, which were most sensitive to relative permeability.

For reservoir oils, the depletion recovery of surface oil initially increases with increasing initial gas–oil ratio. Oil recovery reaches a maximum for moderate-GOR oil reservoirs, followed by decreasing oil recoveries with increasing initial solution GOR. A minimum oil recovery is reached at a near-critical oil. For gas reservoirs, depletion drive condensate recovery increases monotonically from a near-critical gas towards near 100% condensate recovery for very-high GOR systems.

STO recovery from oil reservoirs depends increasingly on gas–oil relative permeabilities as initial solution GOR increases, up to a point. At higher initial solution GORs, oil recovery becomes less dependent on relative permeability and, as the fluid system transitions to a gas at the critical point, relative permeability dependence rapidly diminishes. Condensate recovery from

☆ This paper was prepared for presentation at the 10th Annual India Oil and Gas Review Symposium and International Exhibition, Mumbai, India, September 8–9, 2003.

* Corresponding author.
E-mail addresses: singh@pera.no (K. Singh), fevang@pera.no (Ø. Fevang), curtis@ipt.ntnu.no (C.H. Whitson).

doi:10.1016/j.petrol.2005.01.008

gas condensate systems is more or less independent of gas–oil relative permeabilities, with only slight dependence for near-critical gases.

Keywords: Depletion; Oil recovery; Gas–oil

1. Introduction

1.1. Depletion recovery mechanisms

Primary recovery is classified by one or more of the following drive mechanisms—internal depletion, gascap expansion, aquifer influx, and compaction.

Internal depletion describes the behavior of a single-phase oil or gas fluid system expanding during pressure decline caused by production. Above the initial saturation pressure, the expansion is given by the initial system's total (fluid+pore) compressibility. Below the saturation pressure, both gas and oil phase amounts, compressibilities, and mobilities dictate performance.

Gascap expansion applies to an oil reservoir containing an overlying gas cap. Production from the oil zone causes a pressure drop, which in turn causes the gas cap to expand. The expanded gas sweeps into the oil zone and provides pressure support.

Water influx from an aquifer reacts to pressure drop from the hydrocarbon reservoir, providing a sweep of the hydrocarbons and pressure support.

For a single-volume reservoir,[1] the depletion performance as reflected by oil recovery and pressure decline is dependent on: (a) initial pore volumes of gas, oil, and water associated with the reservoir; (b) fluid and pore compressibilities; (c) changes in phase volumes within the reservoir during depletion, primarily caused by expansion and gas–oil phase splitting below saturation pressure; and (d) changes in relative mobilities of each phase as dictated by relative permeabilities. It is extremely difficult to quantify the impact of each effect on depletion performance, although we generally use geologic, core, PVT, pressure transient, and rate-decline data to estimate their individual contributions.

1.2. Fluid systems

Internal depletion performance depends strongly on reservoir fluid properties. Reservoir fluids are classified as *black oil*, *volatile oil*, *gas condensate*, *wet gas*, and *dry gas* on the basis of saturation type at reservoir temperature and first stage separator conditions (Whitson and Brule, 2000; McCain, 1988). Reservoir fluids can be loosely identified on the basis of initial solution GOR: black oil GOR <200 S m^3/S m^3, volatile oil GOR from 200 to 500 S m^3/S m^3, gas condensate GOR from 500 to 2500 S m^3/S m^3, wet gas GOR from 2500 to 10,000 S m^3/S m^3, and dry gas GOR, effectively infinite.

1.3. Internal depletion behavior

Above the initial saturation pressure of the fluid system, pressure decline is dictated by compressibilities of the hydrocarbon, water, and porous rock. For most oils and gases at high pressure, hydrocarbon compressibility may be similar to pore and water compressibilities; total system compressibilities on the order of 15–45E−5 per bar are characteristic for such low-compressibility systems, with rapid pressure depletion experience after relatively low recoveries.

For reservoir oils producing below the initial bubblepoint, gas comes out of solution. The resulting total system compressibility increases dramatically and the pressure decline slows significantly (Fig. 1). The efficiency of oil recovery (oil recovery percent per bar pressure decline) is highest below the bubblepoint and before gas gains mobility. The pressure decline actually becomes concave upwards before gas gains mobility, as all gas coming out of solution experiences an increasing gas compressibil-

[1] A single-volume reservoir is defined as a reservoir unit in pressure and flow communication, without significant barriers to flow.

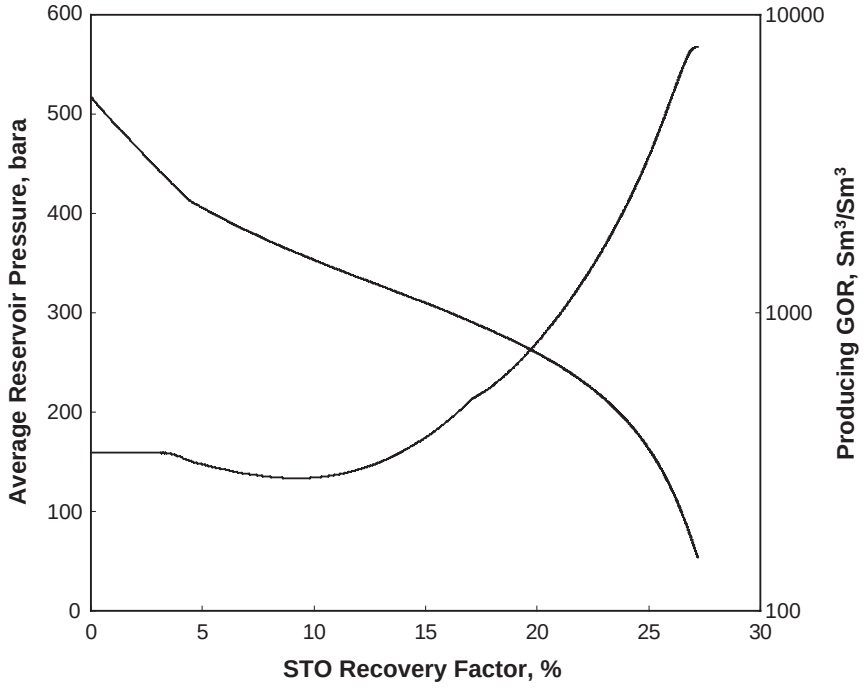

Fig. 1. Depletion oil reservoir performance—variation of reservoir pressure and producing gas–oil ratio with production.

ity. When gas gains mobility and starts producing, the net total system compressibility decreases and pressure decline accelerates. The rate at which gas gains mobility is controlled by critical gas saturation and the $k_{rg}/k_{ro}(S_g)$ relationship for $S_g > S_{gc}$ (Fevang and Whitson, 1996).

For gas condensates, recovery of surface oil (condensate) is controlled by how much of the initial condensate remains in solution as pressure drops below the dewpoint. The retrograde condensate which buildups in the reservoir is immobile for practical purposes.[2]

1.4. Well performance

Well performance is calculated by a rate equation relating surface rates with pressure drawdown (pressure difference between average reservoir and bottomhole flowing pressures). In an oil reservoir above the bubblepoint, only single phase oil flows in the reservoir and rate is directly proportional with drawdown. When BHFP drops below the bubblepoint, oil mobility near the well drops and the oil productivity drops, usually expressed by a rate equation with oil rate proportional with pressure-squared drop (Vogel, 1968; Fetkovich).

For gas condensates with BHFP about the initial dewpoint, the rate equation is as originally proposed by Al-Hussainy et al. (1966). When BHFP drops below the dewpoint, a two-phase gas–oil steady-state flow region develops near the well, and gas relative permeability drops by a factor of 2–20 (near-well k_{rg} from 0.5 to 0.05). This translates into a condensate blockage skin with a magnitude of 5–50. Condensate blockage correlates strongly with producing GOR, where the impact is most severe for low-GOR condensate wells.

1.5. Modeling study

This paper considers only natural depletion of a single-phase hydrocarbon mixture with composition

[2] Near the well out to a few hundred feet, condensate saturation may build up to relatively high values (30–60%). However, this near-well condensate volume represents only a very small fraction of the initial condensate in place and has essentially no effect on ultimate recovery.

defined by its initial solution gas–oil ratio. Water influx is ignored. Pore and connate water compressibilities are included but have a negligible effect on most results. A wide range of reservoir fluids has been investigated, with GORs from 35 to 25,000 S m^3/S m^3.

A single black-oil table was used, generated from a critical reservoir fluid mixture described by a cubic equation of state with five C_{7+} fractions. Four gas–oil relative permeability curves were used to show the impact of critical gas saturation and $k_{rg}/k_{ro}(S_g)$ shape on recovery performance.

Single-cell runs were made to establish the oil recovery and pressure performance for each fluid system. These simulations did not consider well performance. A second set of simulations was run using a fine-gridded radial model, where it was found that the oil recovery and average pressure performance were similar to the single-cell runs, but it was possible to assess the impact of two-phase near-well flow behavior on well productivity. Finally, a set of runs was made using typical full-field grid cells to compare the well productivity performance with fine-gridded radial well models (e.g., plateau period).

The fluid data, reservoir data, and simulation models used in this study are described in Appendix A.

2. Reservoir performance analysis

2.1. STO recovery factor

Recovery factor is defined as the ratio of recoverable reserves to initial fluid in place. Recovery factor depends on various parameters such as drive mechanism, fluid, and rock properties (Arps and Roberts; Arps; Muskat and Taylor, 1946).

In this work, STO recovery factors were calculated for reservoir fluids with different initial solution GORs using the single-cell model. First the reservoir was simulated for an oil with an initial solution GOR of 35 S m^3/S m^3. The oil recovery

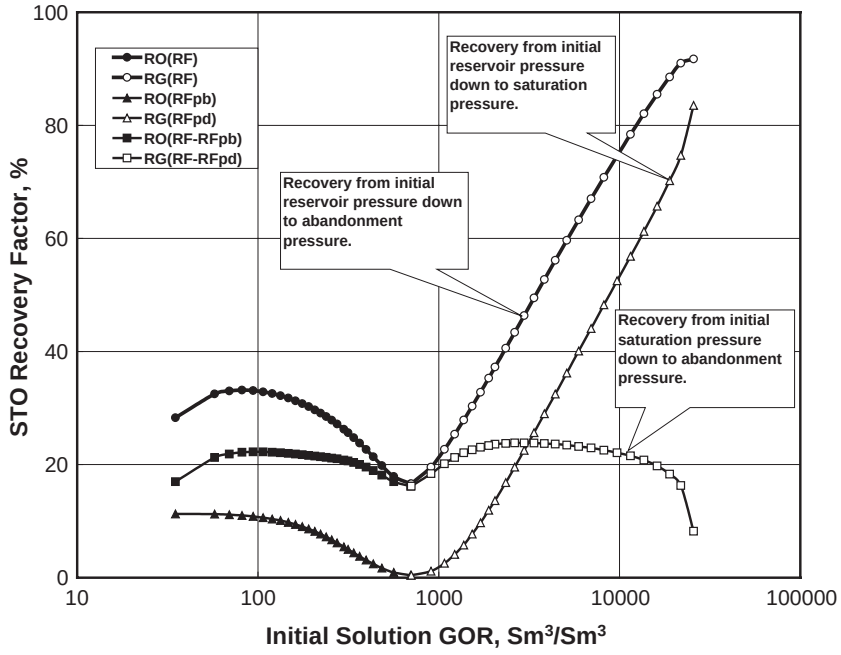

Fig. 2. STO recovery versus initial solution GOR: (a) total oil recovery (i.e., from initial reservoir pressure down to abandonment pressure); (b) from initial reservoir pressure down to saturation pressure; and (c) from saturation pressure to abandonment pressure. The GOR range covers from low-GOR oil to near-critical fluid to rich gas condensate to lean gas condensate.

factor in this case was equal to 28.28%. Recovery factor was calculated for reservoir oils with different initial solution GORs. Simulated STO recovery factor (from initial reservoir pressure down to abandonment pressure) versus initial solution GOR is plotted in Fig. 2. The recovery of STO first increases with increasing initial solution GOR and reaches a maximum value at initial solution GOR of around 100 S m^3/S m^3. Then the recovery factor decreases as initial solution GOR increases and reaches a minimum value of 16% for the near-critical oil.

For gas reservoirs, STO recovery was 91.73 % for reservoir gas with initial solution GOR of 25695 S m^3/S m^3. Recovery factors are plotted in Fig. 2 for gas reservoirs with different initial solution GORs. STO recovery factor increases monotonically with increasing initial solution GOR for gas reservoirs.

Recovery was split in two parts: from initial reservoir pressure to saturation pressure, and from saturation pressure to abandonment pressure. Low-GOR oil reservoir is more undersaturated as shown in Fig. 3. Consequently the recovery from initial reservoir pressure down to saturation pressure is higher due to simple expansion of reservoir fluid as shown in Fig. 2. As saturation pressure increases, the reservoir fluid becomes less undersaturated. For near-critical oil reservoir, the saturation pressure is close to the initial reservoir pressure so recovery down to the saturation pressure is almost negligible. Recovery from saturation pressure to abandonment pressure first increases with increasing initial solution GOR and then decreases.

For near-critical gas, recovery from initial reservoir pressure down to saturation pressure is negligible since initial reservoir pressure is close to saturation pressure. As the reservoir fluid becomes more undersaturated with decreasing initial solution GOR, the oil recovery down to saturation pressure increases as shown in Fig. 2. This is due to the fact that high STO recovery is obtained before reservoir pressure reaches saturation pressure.

To evaluate the effect of relative permeabilities on STO recovery, three different sets of relative

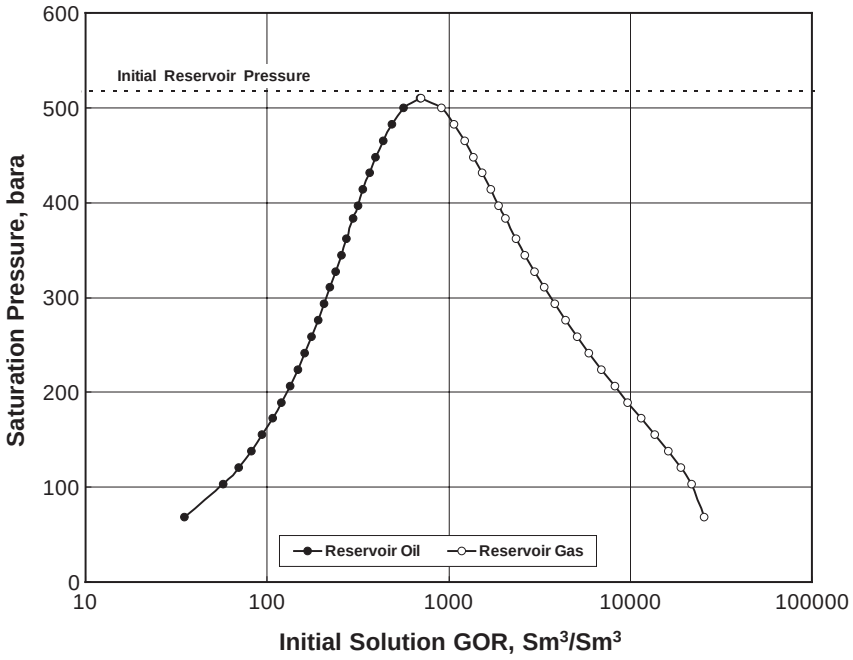

Fig. 3. Saturation pressure versus initial solution GOR. The bubblepoint pressure of oil increases with increasing solution GOR. The dewpoint pressure of gas decreases with increasing initial solution GOR.

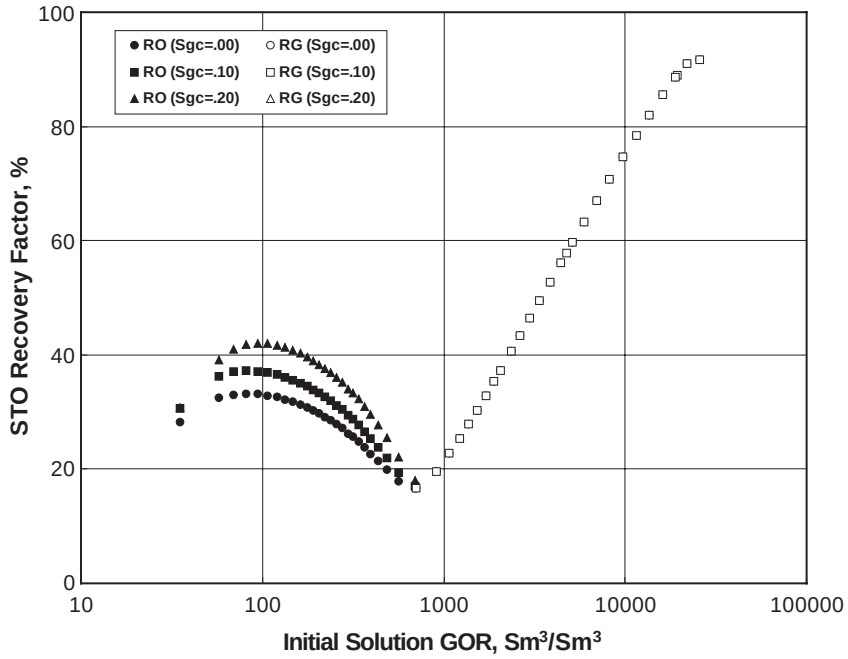

Fig. 4. Effect of critical gas saturation on STO recovery for oil and gas reservoirs.

permeabilities generated with critical gas saturation of 0.0, 0.10, and 0.20 were used in the simulation (Figs. A7 and A8). Gas liberated from the oil remains in the reservoir until critical gas saturation is reached. STO recovery is higher with a high critical gas saturation as shown in Fig. 4. For gas reservoirs, there is no change in STO recoveries with critical gas saturation as shown in Fig. 4.

3. Plateau production rate

For a 5-year plateau production period, plateau oil rate from oil reservoirs and plateau gas rates from gas reservoirs were calculated for different initial solution GORs using different simulation models.

The single-cell model was used for calculating plateau production rate for different initial solution GORs. The plateau oil production rate for oil reservoirs and plateau gas production rates for gas reservoirs are shown in Fig. 5.

For oil reservoirs, plateau oil rate increases with increasing initial solution GOR and reaches a maximum at solution GOR of 150 S m^3/S m^3. The maximum plateau rate coincided with the reservoir fluid that reached a gas saturation close to the critical gas saturation at the end of plateau period. For low-GOR oils, free gas is produced after more than 5 years of production. For high-GOR oils, free gas is produced before 5 years of production. For gas reservoirs, plateau gas production rate increases with increasing initial solution GOR as shown in Fig. 5.

Plateau production rates were also calculated using fine-grid radial model and are shown in Fig. 5. The plateau production rate is lower from the radial model than from the single-cell model due to the method used by the numerical simulator to calculate production rate for the well grid cell (Whitson and Fevang, 1997).

4. Plateau production period

The plateau production rate (for a plateau period of 5 years) from the fine-grid model was used in the coarse-grid model as plateau production rate. Plateau production period was calculated using different coarse-grid models. The comparative plateau periods for different initial solution GORs are shown in Fig. 6.

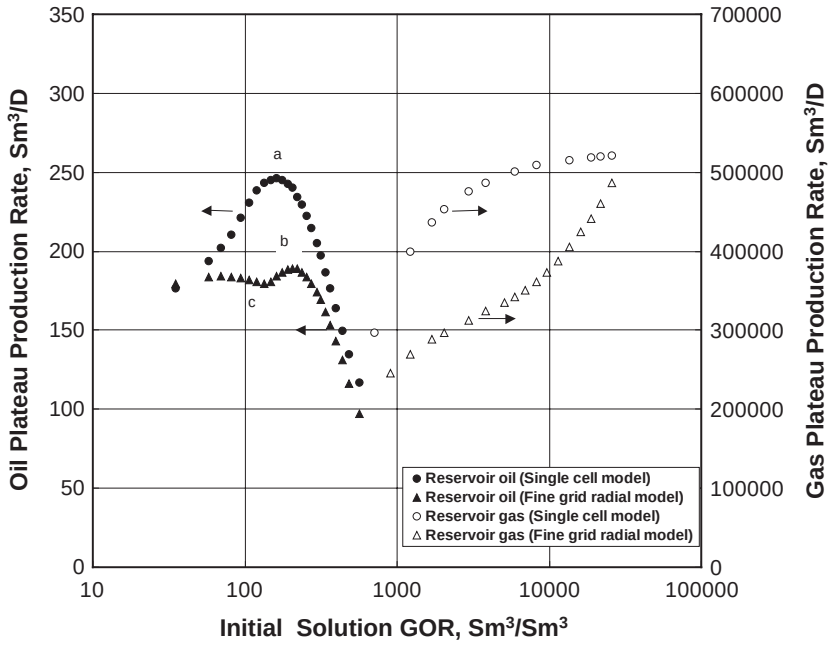

Fig. 5. Plateau oil/gas production rate (5 years of plateau period) versus initial solution GOR. Plateau oil rate for oil reservoirs and plateau gas rate for the gas reservoirs (single-cell and fine-grid radial models).

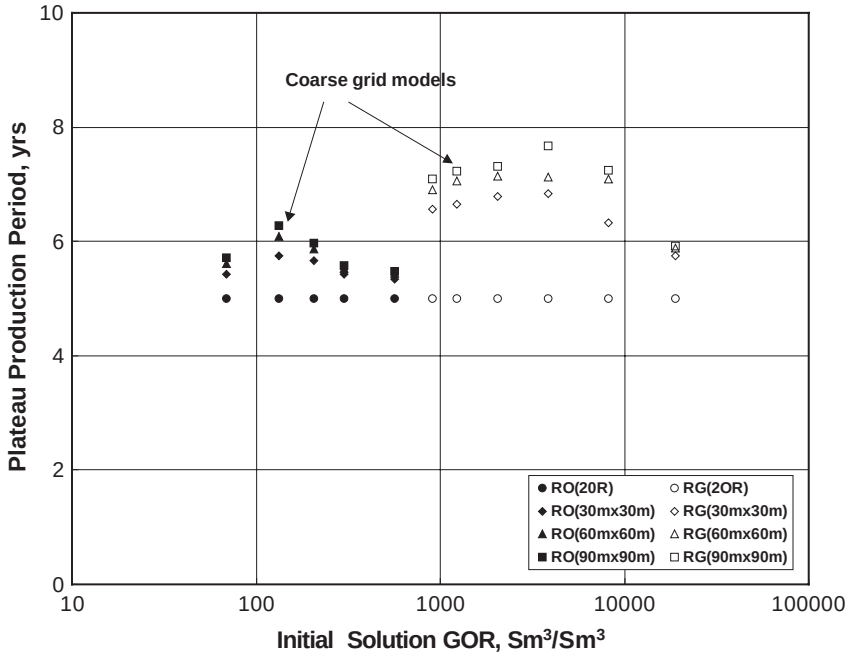

Fig. 6. Comparison of plateau period (a) fine-grid radial model (20R) and (b) coarse-grid models. Plateau period for fine-grid radial model is 5 years.

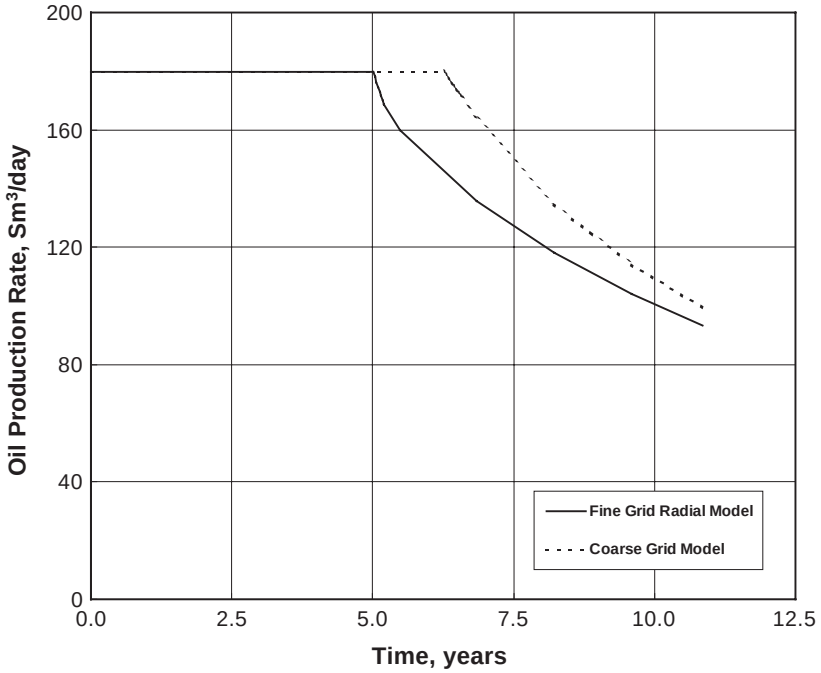

Fig. 7. Comparison of oil production rate for (a) fine-grid radial model and (b) coarse-grid model (90 m×90 m×30 m).

The plateau period is overpredicted in coarse-grid model for both oil and gas reservoirs, about 40% for gas reservoirs and 20% for oil reservoirs. The plateau period difference in fine-grid radial and coarse-grid model reduces with reducing grid size in coarse-grid model. A comparative oil production rate from the fine-grid radial model and coarse-grid model is shown in Fig. 7.

5. Conclusions

This study provides general depletion performance behavior for a wide range of reservoir fluids from black oil through critical mixtures to lean gas condensates. The reservoir is considered a single geologic unit without flow barriers; water influx is ignored. Surface oil recovery includes condensate recovery.

1. For oil reservoirs, the recovery of surface oil increases with increasing initial solution GOR until a moderate GOR of about 100 S m^3/S m^3 where a maximum recovery level of 30–40% was reached. At higher GORs, the oil recovery decreased monotonically towards a minimum of about 16% at the GOR of 700 S m^3/S m^3 where the fluid becomes critical and transitions into a gas system.
2. For gas reservoirs, the surface condensate recovery increases monotonically from about 16% for the near-critical gas system with 700 S m^3/S m^3 GOR towards very high recoveries (approaching surface gas recovery factors) for very-lean high-GOR systems.
3. Other than the initial solution GOR of the system, the second most important factor influencing oil recovery was the gas–oil relative permeability curve $k_{rg}/k_{ro}(S_g)$ and critical gas saturation S_{gc}. Relative permeability has the greatest effect on oil systems with a GOR near 100 S m^3/S m^3, resulting in a range of maximum oil recoveries from 30% to 40% for *poor* to *excellent* relative permeability curves, respectively.
4. Relative permeability curves had essentially no effect on condensate recoveries, even for the

near-critical rich condensate with initial solution GOR of 700 S m^3/S m^3 (r_{si} of 1400 S m^3/1E6 S m^3).

5. For an oil well producing with constant rate constraint for a fixed period of time (e.g., 5 years), the plateau oil rate is a maximum for an initial solution GOR of about 200–250 S m^3/S m^3. This is somewhat higher than the GOR of 100 S m^3/S m^3 with maximum ultimate oil recovery factor. The plateau oil rate is more or less constant and only slightly less (than the 'optimal' oil rate) for initial solution GORs lower than 250 S m^3/S m^3. However, at higher initial solution GORs, the plateau oil rate drops steadily as GOR approaches 700 S m^3/S m^3 where the oil rate is less by a factor of 2.
6. For a gas well producing with constant rate constraint for a fixed period of time (e.g., 5 years), the plateau gas rate monotonically increases for systems with increasing initial solution GOR. Clearly the effect of blockage is decreasing for leaner produced gas condensate mixtures.
7. Compared with fine-grid radial model results, the error in predicted plateau period using a typical full-field coarse-grid model and standard well productivity treatment is worst for gas condensates. The error is equally bad (about 40% overpredicted plateau period) for initial solution GORs from 1000 to 10,000 S m^3/S m^3. Little difference was found in predicted plateau periods for near-critical gases and volatile oils, while a 20% overpredicted plateau period was found for oils with initial solution GORs of about 100–200 S m^3/S m^3.

Nomenclature

B_{gd}	Dry gas FVF, R m^3/S m^3
B_o	Oil FVF, R m^3/S m^3
R_s	Solution gas–oil ratio, S m^3/S m^3
r_s	Solution oil–gas ratio, S m^3/S m^3
k_{rg}	Gas relative permeability
k_{ro}	Oil relative permeability
S_g	Gas saturation
S_{gc}	Critical gas saturation
GOR	Gas–oil ratio, S m^3/S m^3
OGR	Oil–gas ratio, S m^3/S m^3
RO	Reservoir oil
RG	Reservoir gas
RF	Recovery factor
RF_{pb}	Recovery factor from initial reservoir pressure to bubblepoint
RF_{pd}	Recovery factor from initial reservoir pressure to dewpoint
MB	Single-cell material balance model
STO	Stock-tank oil
20R	Fine-grid radial grid model with 20 grids in radial direction

Acknowledgement

We would like to acknowledge NORAD (Norwegian Agency for International Development) for providing financial support during this research work. Many thanks to the staff of the Department of Petroleum Engineering and Applied Geophysics, NTNU, especially to Kathy Herje, for the assistance and support rendered during the study.

Appendix A. Fluid and reservoir data

A.1. PVT data

Reservoir fluid properties have been generated using the Peng–Robinson equation of state with five C_{7+} fractions. A mixture was created by recombining separator oil and gas samples with a GOR of approximately 700 S m^3/S m^3. This mixture had a critical point of 510 bar at 130 °C. Depletion of the critical mixture using a CCE experiment (Fevang et al., 2000) resulted in black-oil properties, which could be used to describe a wide range of reservoir fluids from oils with GOR down to 35 S m^3/S m^3 to lean gases with GOR up to 25,000 S m^3/S m^3. Generated saturated and undersaturated PVT properties are shown in Figs. A1–6 and saturated PVT properties are given in Table 1.

A.2. Relative permeabilities

Relative permeabilities were generated using Corey correlation (Standing, 1975; Chierici, 1984). Four different sets of relative permeabilities were generated using different critical gas saturations (i.e., 0.0, 0.01, 0.1, and 0.2). Relative permeability with

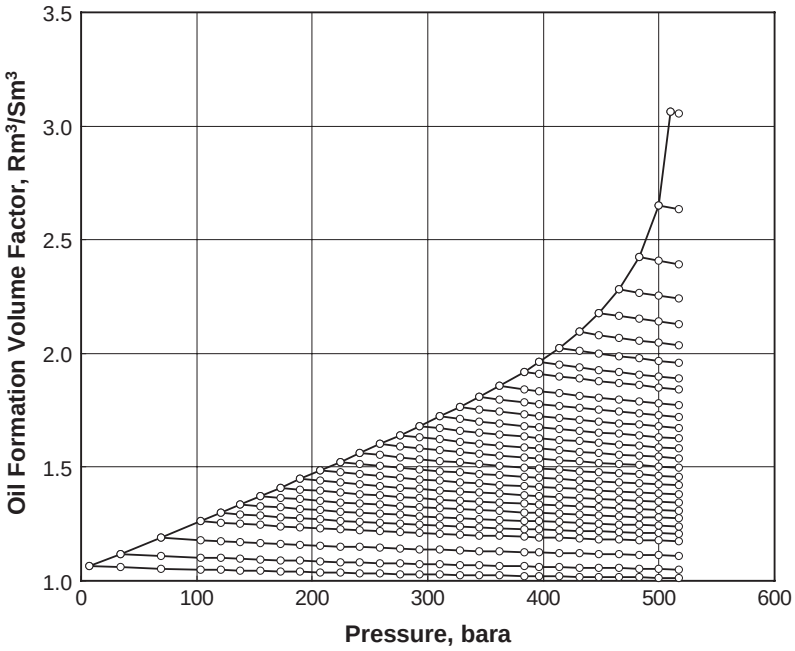

Fig. A1. Saturated and undersaturated oil formation volume factor versus pressure.

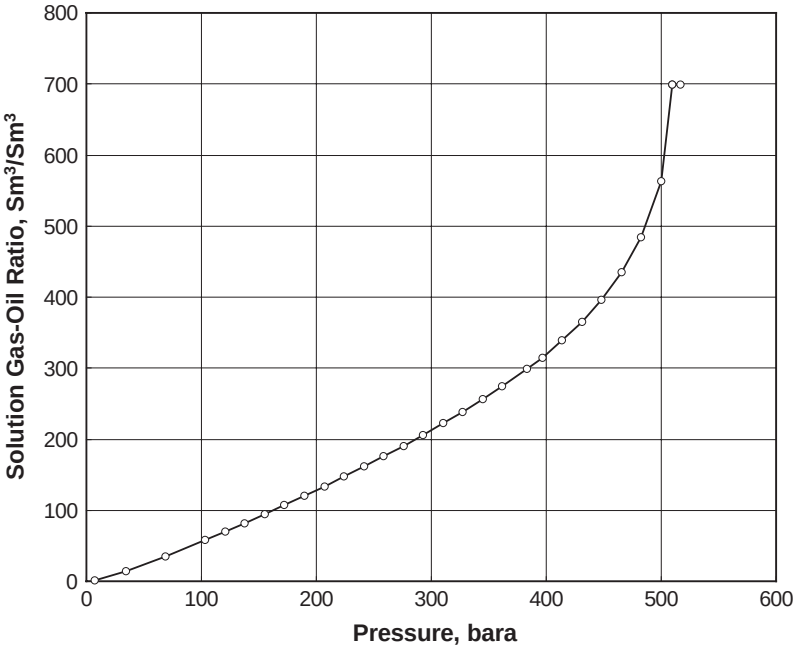

Fig. A2. Solution gas–oil ratio versus pressure.

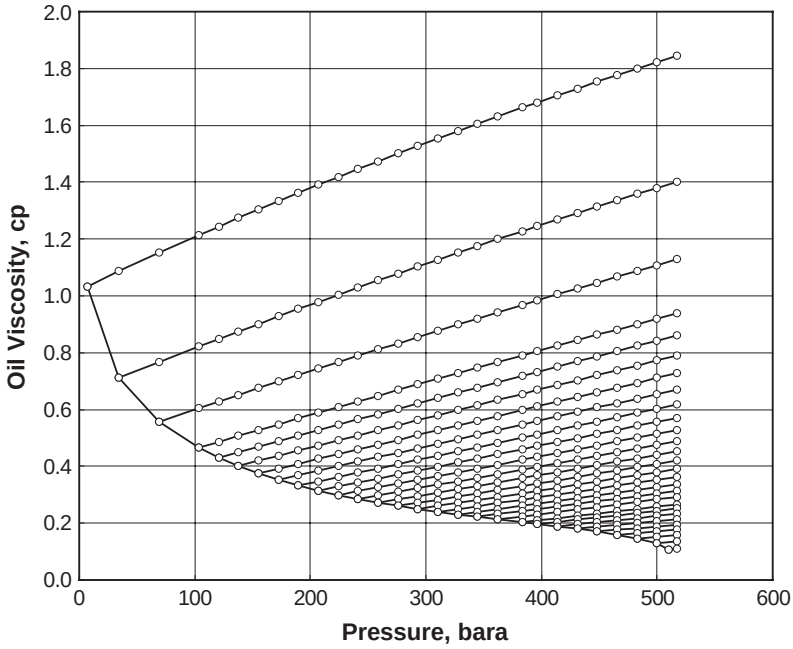

Fig. A3. Saturated and undersaturated oil viscosities versus pressure.

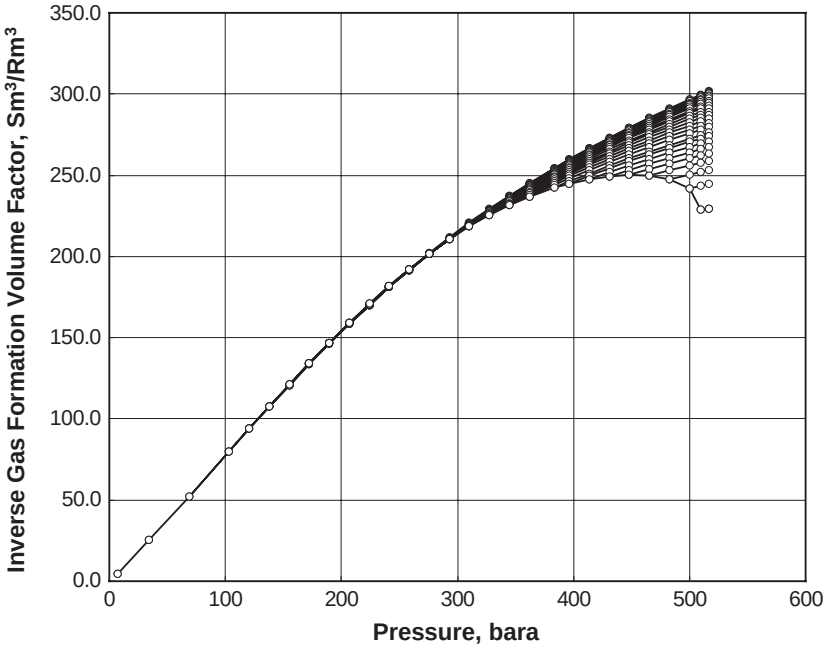

Fig. A4. Saturated and undersaturated gas formation volume factor versus pressure.

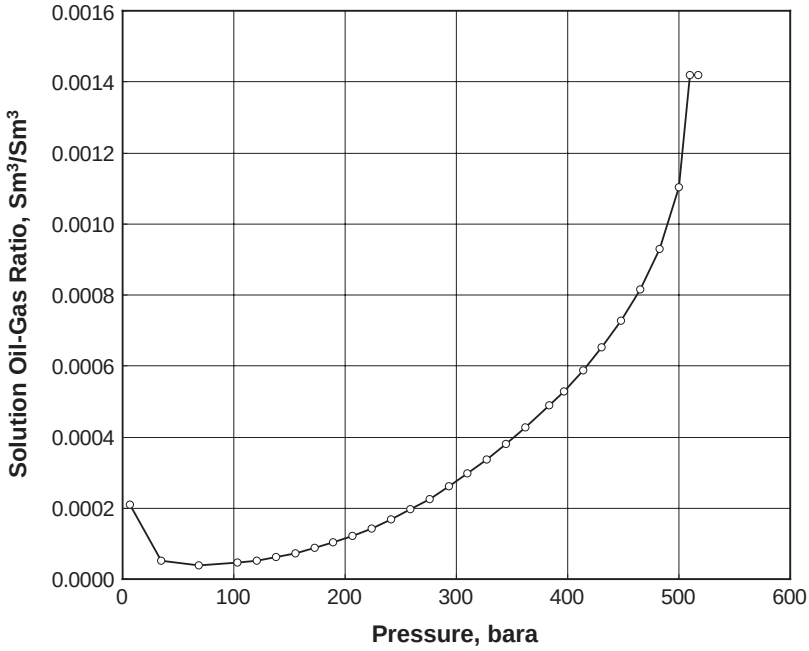

Fig. A5. Solution oil–gas ratio versus pressure.

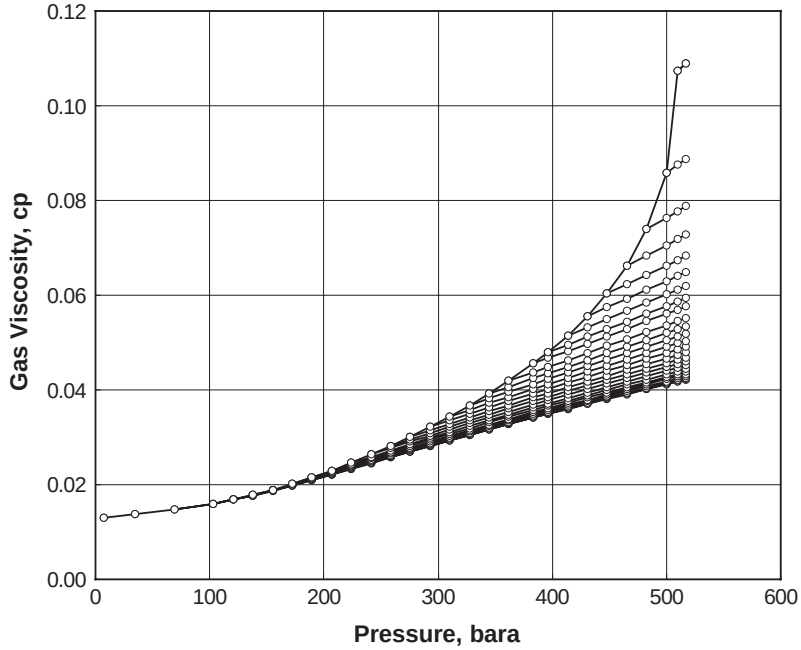

Fig. A6. Saturated and undersaturated gas viscosities versus pressure.

Table 1
Saturated black-oil PVT properties

Pressure (bara)	Solution gas–oil ratio (S m^3/S m^3)	Solution oil–gas ratio (S m^3/S m^3)	Oil formation volume factor (R m^3/S m^3)	Oil viscosity (cP)	Gas formation volume factor (R m^3/S m^3)	Gas viscosity (cP)
7	1.3	0.000211	1.0644	1.0336	0.20939	0.0130
34	14.3	0.000052	1.1189	0.7115	0.03950	0.0137
69	35.0	0.000039	1.1903	0.5577	0.01913	0.0147
103	57.6	0.000046	1.2629	0.4658	0.01252	0.0160
121	69.4	0.000053	1.2994	0.4310	0.01067	0.0168
138	81.6	0.000062	1.3360	0.4012	0.00930	0.0178
155	94.1	0.000073	1.3729	0.3753	0.00827	0.0189
172	106.8	0.000087	1.4099	0.3527	0.00745	0.0201
190	120.0	0.000103	1.4473	0.3327	0.00681	0.0215
207	133.4	0.000122	1.4850	0.3150	0.00628	0.0230
224	147.2	0.000144	1.5231	0.2991	0.00585	0.0246
241	161.4	0.000168	1.5617	0.2850	0.00550	0.0263
259	175.9	0.000196	1.6008	0.2722	0.00520	0.0282
276	190.9	0.000226	1.6404	0.2606	0.00496	0.0301
293	206.2	0.000260	1.6808	0.2501	0.00475	0.0322
310	222.1	0.000297	1.7222	0.2404	0.00458	0.0344
328	238.6	0.000337	1.7649	0.2314	0.00444	0.0368
345	255.9	0.000380	1.8094	0.2227	0.00432	0.0392
362	274.1	0.000426	1.8564	0.2144	0.00422	0.0419
383	298.7	0.000488	1.9200	0.2041	0.00413	0.0456
396	315.0	0.000529	1.9623	0.1978	0.00408	0.0480
414	338.5	0.000588	2.0240	0.1891	0.00404	0.0515
431	365.2	0.000653	2.0948	0.1801	0.00401	0.0556
448	396.4	0.000728	2.1786	0.1703	0.00400	0.0604
465	434.4	0.000816	2.2827	0.1595	0.00400	0.0662
483	484.4	0.000929	2.4227	0.1469	0.00404	0.0739
500	563.5	0.001103	2.6512	0.1301	0.00413	0.0859
510	699.4	0.001418	3.0646	0.1081	0.00437	0.1073

critical gas saturation of 0.0 was used for STO recovery factor calculation, and 0.01 was used for plateau rate and plateau period calculation. Other relative permeabilities were used to study the effect of relative permeabilities on recovery. The oil and gas relative permeabilities are shown in Figs. A7 and A8.

A.3. Reservoir properties

Reservoir rock porosity is 0.30 and permeability is 5 md. Initial reservoir pressure is 517 bar for all the cases. Thickness of the layer is 30 m. Other reservoir properties are given in Table 2. The reservoir is produced through one well controlled on maximum withdrawal rate and a minimum well bottomhole flowing pressure of 35 bar. The producer is located in the center of the reservoir and the economic limit is 0.1 S m^3/D.

A.4. Reservoir simulation models

Reservoir simulation study was done using a black-oil numerical reservoir simulator (Eclipse 100a,b). Single-cell material balance model, two-dimensional radial model, and three-dimensional coarse-grid models were used in the simulation study.

In the single-cell material balance model, only one grid cell was used with a radius of 450 m and a thickness of 30 m. The fine-grid radial model contains 20 grid cells in the radial direction and one grid cell in the vertical direction. The grid cell thickness in radial direction increases in such a way that the ratio of the radius of two consecutive grids is the same. Reservoir pore volume in the fine-grid radial model was the same as in the single-cell model.

Grid cell size in the coarse-grid Cartesian model is 90 m×90 m×30 m. Grid cell sizes in other coarse-

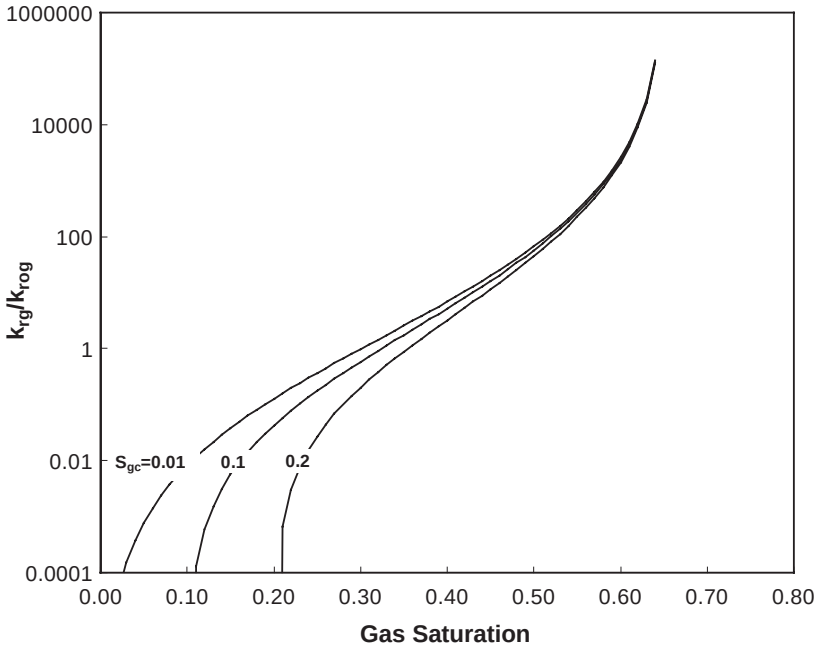

Fig. A7. Ratio of k_{rg}/k_{rog} versus gas saturation for different critical gas saturations.

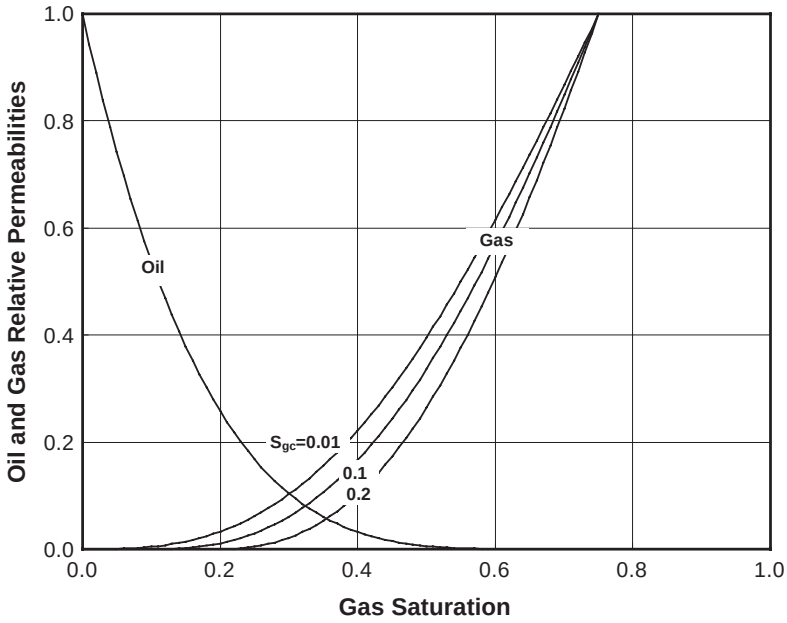

Fig. A8. Oil and gas relative permeabilities versus gas saturation for different critical gas saturations.

Table 2
Basic reservoir properties

Reservoir external radius, m	450
Reservoir thickness, m	30
Porosity, %	30
Absolute permeability, md	6
Initial reservoir pressure, bar	517
Reservoir temperature, °C	130
Wellbore radius, m	0.11
Minimum bottomhole flowing pressure, bara	35
Irreducible water saturation, %	25
Fine-grid radial model	
Number of grid cells in radial direction	20
Grid cell thickness, m	30
External radius, m	450
Coarse-grid model grid cell size	
(a)	90 m×90 m×30 m
(b)	60 m×60 m×30 m
(c)	30 m×30 m×30 m

grid models are 60 m×60 m×30 m and 30 m×30 m×30 m. The number of grid cells in the coarse-grid models was selected such that the volume of the reservoir was same as in the case of the radial model.

References

Al-Hussainy, R., Ramey Jr., H.J., Crawford, P.B., 1966. The flow of real gases through porous media. JPT, 624.

Arps, J.J., Reasons for differences in recovery efficiency, SPE paper 2068.

Arps, J.J. and Roberts, T.G., The effect of the relative permeability ratio, the oil gravity, and the solution gas–oil ratio on the primary recovery from a depletion type reservoir, Paper presented at the 1955 AIME Annual Meeting (February 13–17), Chicago.

Chierici, G.L., 1984. Novel relations for drainage and imbibition relative permeabilities. SPEJ, SPE Paper, vol. 10165, June.

Eclipse 100, Reference manual.

Eclipse 100, Technical appendices.

Fetkovich, M.J., The isochronal testing of oil wells, Paper SPE 4529 presented at the 1973 SPE Annual Technical Conference and Exhibition, Las Vegas, September 30–October 3.

Fevang, Ø., Whitson, C.H., 1996. Modeling gas condensate well deliverability. SPE Reservoir Engineering, 221 (November).

Fevang, Ø., Singh, K., Whitson, C.H., 2000. Guidelines for choosing compositional and black-oil models for volatile oil and gas-condensate reservoirs. Paper SPE 63087 presented at the 2000 annual technical conference and exhibition, Dallas, Texas, October 1–4.

McCain, W.D., 1988. The Properties of Petroleum Fluids, 2nd ed. PennWell Publishing Co., Tulsa, OK.

Muskat, M., Taylor, M.O., 1946. Effect of reservoir fluid and rock characteristics on production histories of gas drive reservoirs. Trans., AIME 165, 78–93.

Standing, M.B., 1975. Notes on Relative Permeability Relationship. NTNU, Trondheim, Norway.

Vogel, J.V., 1968. Inflow performance relationships for solution–gas drive wells, JPT (January 1968), pp. 83–92; Trans., AIME, p. 243.

Whitson, C.H., Brule, M.R., 2000. Phase Behavior. Monograph Series. SPE, Richardson, TX.

Whitson, C.H., Fevang, Ø., 1997. Generalized pseudopressure well treatment in reservoir simulation. Proceedings of the IBC Conference on Optimisation of Gas Condensate Fields.